TOUGHENING MECHANISMS FOR MONOLITHIC CERAMICS

M.V. Swain

CSIRO Division of Materials Science and Technology

Locked Bag 33, Clatyon, Victoria 3168 Australia

ABSTRACT

The last decade has seen a dramatic improvement in the mechanical properties of structural ceramics. Strengths in excess of 2GPa and fracture toughness values higher than $1KJm^{-2}$ are now possible. These improved properties are possible because of the availability of highly sinterable powders coupled with hot isostatic pressing and the incorporation of new toughening mechanisms such as transformation toughening and fiber and whisker reinforcement. Means of combining more than one mechanism in a specific microstructure are also being developed. The primary role of the most effective troughening mechanisms is to reduce the crack tip stress intensity factor by 'crack tip shielding'. In this manuscript the various mechanisms for toughening are outlined along with examples of materials systems exhibiting this behaviour.

INTRODUCTION

The last decade has seen a tremendous upsurge of interest in ceramics. One of the worries of many old hands in the field is whether this is genuine commitment to this, the oldest of all manufacture commodities or whether it is cyclical market hype. No where has this enthusiasm been more evident than in Japan where "ceramic fever" was diagnosed as early as 1983 . Similar but less ambitious ceramic programs are underway in most technologically advanced nations. The market area with the greatest capacity for growth is considered to be in structural ceramics. Various estimates of the market for structural ceramics have been proposed from 0.1 to 3 x 10^9 US dollars in 1995, with the total ceramic market up to 15 to 20 x 10^9 US dollars [1].

What has lead to this upsurge of interest in ceramics? There have been a number of factors, such as: appreciation of new toughening mechanisms, availability of high purity sinter active powders, concern regarding supply and expense of strategic metallic materials such as cobalt, tungsten, etc, demand for more fuel efficient and lower cost maintenance engines. Interest in this area has tended to coincide with high oil prices. Of all these factors the major potential contributor to rapid growth for structural ceramic growth is the automotive industry, however as many commentators have warned it is somewhat speculative and depends upon future free market competitive forces and the price of energy. A significant increase in energy costs will greatly facilitate the improved demand for ceramics in heat engines, particularly insulating and gas turbine componentary. Other areas such as wear resistant components for valves, tappets, etc, will also find increasing demand when the production cost decreases and volume capacity

increases. In the meantime demand for wear resistant ceramics is finding increasing application in the metal fabrication area (extrusion dies, cutting tools etc.) and chemical/mining/petroleum processing areas (valves, pumps, seals etc.)

In this paper the emphasis will be on the mechanical properties of structural ceramics particularly on the toughening mechanisms of such materials. Tremendous developments in the field of toughening ceramics have taken place over the last fifteen years. These developments have occured on the theoretical, experimental and technological levels in a manner that has been exceptional productive. The concept that conventionally processed polycrystalline ceramic materials could be substantially toughened was most convincingly demonstrated in partially stabilized zirconia (PSZ) ceramics by Garvie et al [2]. This conceptual breakthrough and the subsequent incorporation of a stress induced phase change into many matrices has taken place. More recently the notion of micro-fibre (on single crystal whisker) reinforcement of a brittle matrix has been appreciated. The combination of these mechanisms (transformation and whisker reinforcement) together with other mechanims leading to a hierarchy of toughening proceedures is leading to the development of exceptionally tough and damage tolerant ceramic materials. The basis of most of these toughening mechanisms is that the effective crack driving force experienced by the crack tip is reduced. Ritchie has termed this class of toughening mechanisms "Crack-tip shielding" [3].

The extension of a crack may be considered due to a **crack driving force** and opposed by the **resistance of the microstructure.** The driving force is generally defined by some parameter that quantifies the loading

system, such as the stress intensity factor or path-independent integral J, which is meant to describe the stress and deformation fields about the crack tip. Crack extension is restrained by reducing the driving force or increasing the toughness of the microstructure. Two possible means are possible to increase the resistance or toughness namely increasing the **intrinsic toughness** of the matrix or by reducing the crack driving force by crack tip shielding, that is by a process termed **extrinsic toughening.** The latter is the more usual approach for toughened ceramics because of the inability to modify significantly the yield behaviour of the matrix or the intrinsic low toughness of ceramic materials.

The aim of this paper is to outline in more detail the concept of crack shielding and then to discuss various mechanisms that result in significant extrinsic toughening of ceramic materials. The emphasis will be placed on the physical basis, and limitations and consequences of toughening ceramic materials including the susceptibility of toughened materials, to cyclic fatigue crack extension. Examples of the various toughening mechanisms and combinations of mechanisms will also be presented.

2. BASIS OF ENHANCED MECHANICAL PERFORMANCE

The two major mechanical properties for engineering ceramics are strength and toughness. Other properties that influence strength, wear resistance and thermo-mechanical behaviour include creep behaviour, hardness, thermal expansion and thermal conductivity. These parameters will not receive attention here. For engineering design purposes the major consideration is the strength of the ceramic material. However

unlike metals, ceramic materials do not have a well defined yield stress or ultimate tensile strength but rather fail catastrophically and show a wide scatter of strengths. This has lead to the development of extreme value function statistical analysis, of which the Weibul analysis is one variant, to provide a basis for interpretation of the observations and means of predicting size and stress loading dependence of strength [4]. It has been known for decades that the tensile strength of fibres of glass, sapphire, etc, may have exceptionally high strength (> 2-3 GPa) [5], but display considerable variability in strength as well as being very vulnerable to damage. Contact with dust particles in the atmosphere may result in 80% reduction of strength. This has necessitated coating of high strength fibres with protective layers as applied currently to telecommunication optical fibre links.

Similar approaches have been applied for polishing surfaces for the improvement in strength of polycrystalline ceramics. Any such gains are usually at great expense and considerable inconvenience and are readily removed when the component enters into service. Other problems associated with strength variability are the influence of pre-existing or introduced flaws (<50μms) and the difficulty of NDE techniques to detect such flaws [6]. The relationship between strength, toughness and flaw or defect size in a ceramic is usually written,

$$\sigma = K_{1c}/ Y\sqrt{c} \qquad (1)$$

where σ_f is the breaking stress, c the flaw size, Y a geometric parameter dependent upon flaw shape and location. By improving processing and or polishing the surface after grinding it is possible to

reduce the flaw size and so increase the strength. However, as is well recognised ceramic materials have very low fracture toughness values and are prone to damage. Hence the only approach to improve the service reliability, is to increase the fracture toughness by mechanisms that impart crack tip shielding.

The concept of crack tip shielding, which is also the basis for the high toughness of metallic materials, is that the resistance to crack growth or measured K_{1c} consists of two or more components, the **intrinsic toughness** of the material plus some additional or **extrinsic toughness** component due to a range of possible options, that is

$$K_{1c} = K_1 + K_s \qquad\qquad (2)$$

where K_1 is the intrinsic matrix toughness and K_s is the contribution due to external shielding. This expression is similar to the expression proposed by for metals where K_s would be the equivalent plastic work component which is usually very much greater than the intrinsic toughness [7]. For polycrystalline materials it is difficult to decide upon a K_1 value because of the influence of grain boundaries etc on crack the path. Lawn and colleagues [8,9] are currently attempting to develop analytical approaches that encompass this feature.

An aspect of major significance associated with crack tip shielding concept is that events in the **wake** of the crack tip are the major contributors to increased toughening. Fig. 1 a. A logical consequence of such wake related toughening effects is that with the initiation of a crack, wake toughening mechanisms only develop with crack extension. That is, K_s is a function of crack extension and the material exhibits R-curve behaviour. Equation (2) should be then re-written
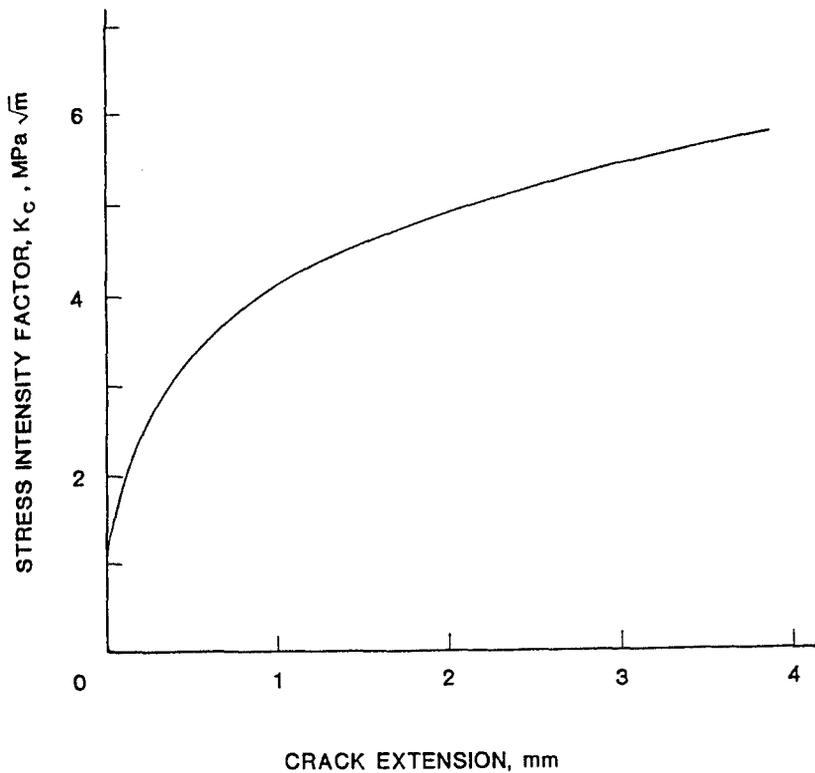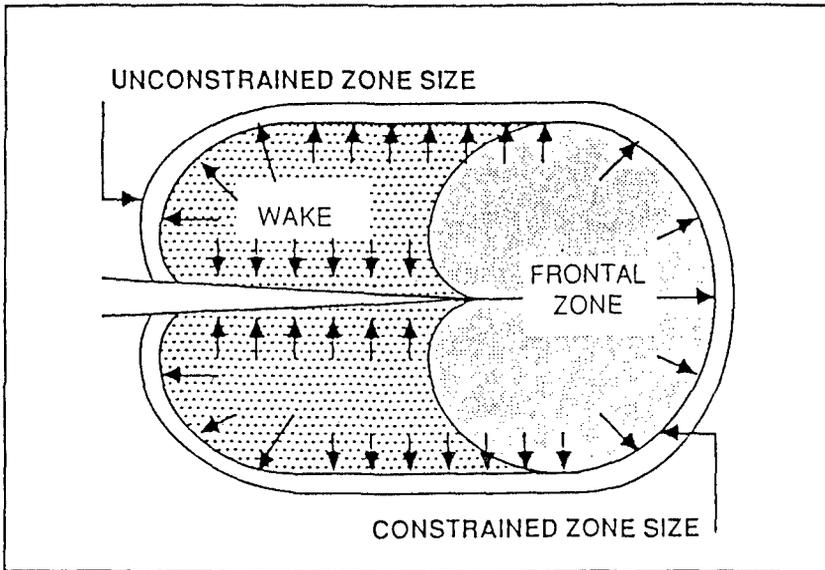
Figure 1. a, Wake region developed about an extending crack.
b, Influence of wake region on toughness.

$$K_{1c} = K_1 + K_s \text{ (c)} \qquad\qquad (3)$$

This consideration is shown schematically in Fig. 1b.

The simple relationship between strength and toughness is now more complex for materials exhibiting crack tip shielding or R-curve behaviour. This situation may be readily appreciated with the aid of Figure 2. A consequence of an R-curve is that the crack becomes unstable when the rate of change of strain energy G with crack length exceeds the rate of change of crack resistance,

$$\frac{dG}{da} \gtrsim \frac{dR}{da} . \qquad\qquad (4)$$

Figure 2 [10,11]. Even this approach is somewhat simplistic as the form of the R-curve will be dependent upon the geometry of the wake, that is one might expect the R-curve for a surface crack to be different from an internal defact or through thickness crack. This feature will be taken up in the final section.

Whilst the consequences of R-curve behaviour are that lower strengths are experienced than anticipated by equation 1, less sensitivity of the strength on initial flaw size (i.e. higher Weibull modulus) is observed. This aspect was originally proposed by Kendall et al [12] and more recently extended by Cook and Clark [13]. Previous studies by Cook et al [14] had established that coarse grained alumina ceramics with significant R-curves were more damage tolerant to Vickers
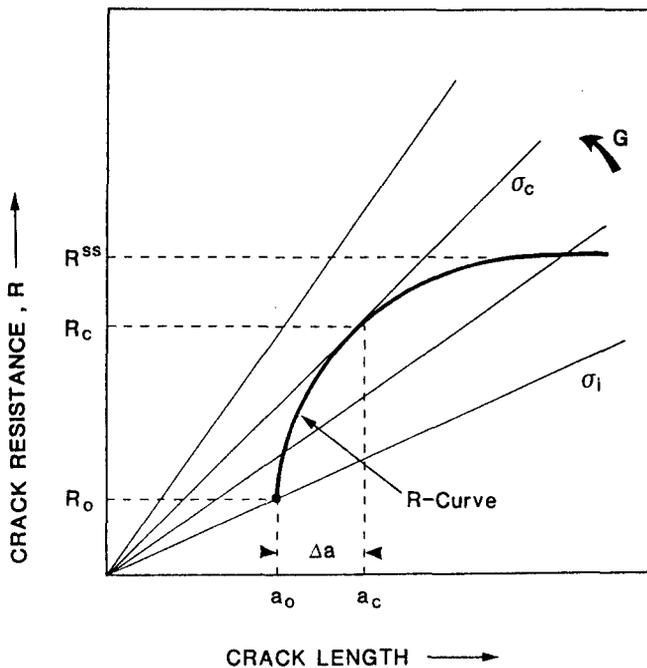
Figure 2. Schematic plot of crack stability due to R-curve response of a material. Crack resistance (R) is plotted on the same figure as the applied strain energy release rate G, equ (3). Crack initiation commences at a stress σ_i when $G = R_c$ and catastrophic failure occurs at a stress σ_c when $G = R_c$ which is less than the steady state toughness R^{ss}.
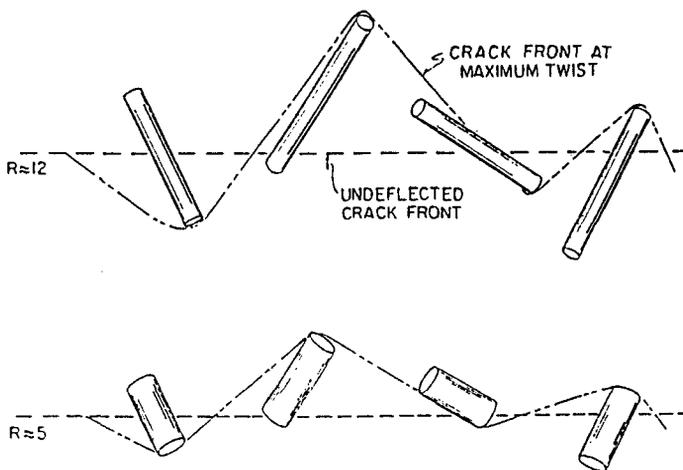

Figure 3. Schematic of crack front deflection and twisting about rods in a matrix. R is the aspect ratio of the rods.

indentation than stronger finer grained alumina. It is also known that R-curve behaviour is beneficial to minimise thermal shock damage [15].

Various micro-mechanisms of crack tip shielding that impart increased toughness and associated R-curve behaviour are listed below characterised into several classes [3,10,16]. These include,

1. Crack deflection and meandering,

2. Zone shielding

    - Residual stress

    - Microcracking toughening

    - Transformation toughening,

3. Contact shielding

    - Crack bridging

    - Whisker and fibre reinforcement.

In the following section each of these classes will be dealt with in some detail along with the anticipated and where available examples illustrating the efficiency and range of there mechanisms. Certain systems have been developed that combine more that one specific shielding effect. This will most certainly be the direction for future research, namely the development of tailored microstructures that optimise the strengthening and toughening increments available via the above and other yet to be appreciated mechanisms.

3 TOUGHENING MECHANISMS

   3.1 Crack Deflection and meandering

Cracks may be deflected from their planar path by a variety of means including; grain boundaries, fracture resistant second phase

particles or residual stresses. A schematic diagram illustrating this mechanism is shown in Figure 3. The basis for the increased toughness associated with this mechanism is that reorientation of the crack plane away from normal to the applied tension causes a reduction in the crack driving force or crack tip stress intensity factor (K). Faber and Evans [17,18] have distingiushed two types of crack deflection: crack tilting about an axis parallel to the crack front, and twisting of the crack plane about on axis normal to the crack front. Fracture mechanics analysis suggests that the twisting component contributes most to the increased toughness.

The toughness increment possible with this mechanism is highly dependent upon the nature of the crack deflection and particulate phase that causes it. The toughening derived from randomly oriented, deflecting particles depends only on the volume fraction and shape of the particles. Rod shaped particles with large aspect ratio contribute maximum toughening because of their influence on the twist angle. The predicted toughening effect of rod shaped particles with different aspect ratio (R) is shown in Figure 4. The interesting feature of this graph is that toughening saturates with relatively low volume fractions of second phase particles. Another important feature about this mechanism is its independence of temperature and particles size.

Examples of materials with microstructures developed to enhance the toughness by this crack deflection mechanism are beginning to appear. Faber and Evans [18] showed this mechanism was relevant in SiC, Si_3N_4 and a glass ceramic materials. Lange [19] demonstrated the improved toughness of Si_3N_4 with increased accicular β phase present. A recent study by Hori et al [20] has clearly demonstrated the effect of volume
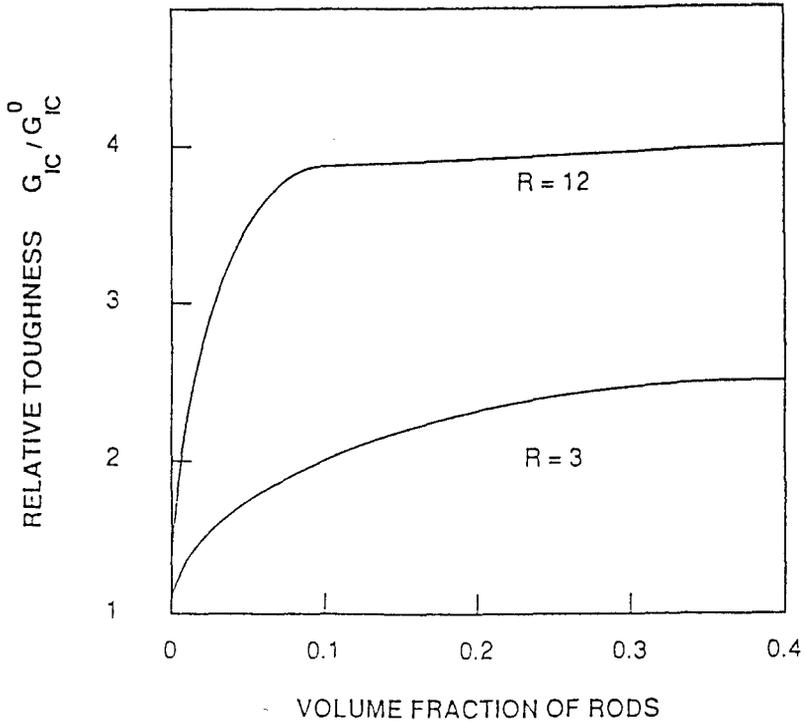
Figure 4. Toughening increment due to crack deflection as a function of volume fraction and aspect ratio of crack deflecting particles.
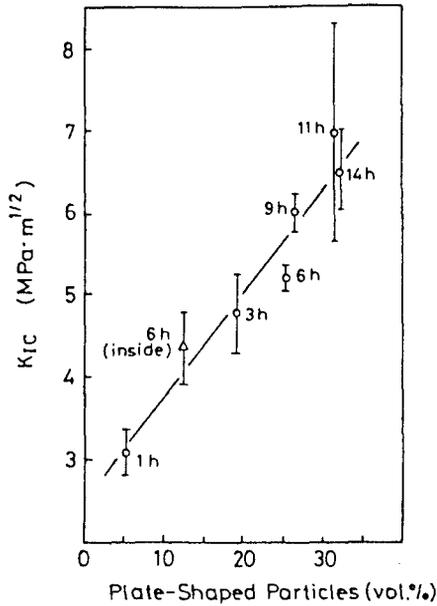

Figure 5. Observations of the toughening effect of plate like particles in a rutile–corundum composite material [20].

fraction of plate like particles in a rutile-corundum composite material. Observations from Hori et al are shown in Figure 5. This mechanism of toughness enhancement will also be considered in the remaining two subsections.

3. 2 Zone Shielding

Mechanisms that provide zone shielding are usually extrinsic toughening mechanisms that reduce the apparent applied stress intensity at the crack tip to the intrinsic toughness of the material. These include: i) the presence of residual stress over a scale much larger than the strength controlling defect sizes, ii) microcrack toughening, and iii) transformation toughening. These three mechanisms will now be considered in greater detail.

3.2.1. Residual Stress

This approach has been recognised for many decades and technologically finds wide application in the glass industry. By thermal quenching glass heated above the softening temperature or chemical ion-exchange tempering, considerable improvements in strength and reduction in their sensitivity to surface damage. In this manner surface compressive stress and compensating internal tensile stresses are developed. Upon the application of a flexural stress these surface compressive tempering stresses must first be overcome before the surface flaws are placed in tension – this might be considered apparent toughening. One obvious disadvantage of this mechanism is that the internal tensile stresses may lead to the spontaneous fracture of glass plates due to inclusions or pre-existing flaws [21].

Need to include expression for apparent toughening based upon Lawn and Marshall's analysis. A detailed analysis of the "effective" toughening associated with a residual tempering stress has been made by Lawn and Marshall [22]. These authors used the scaling porometers of the relative tempering depth d and a modifying factor that scaled with crack depth to tempering zone depth, namely

$$K_s(c) = M(c/d) \; \sigma_R \; (\pi d^{\frac{1}{2}}) \tag{5}$$

where M (cd) is the dimensionless modifying factor that is determined by the tempering stress profile, σ_R is the surface compressive stress and d is the depth of the tempered zone.

Compressive surface stresses can be developed in ceramic materials by several mechanisms. These include thermal tempering as shown by Kirchener et al [23] for polycrystalline alumina, usually containing a glass phase. Volume changes of silicon nitride surfaces by oxidation have also been found to produce surface compressive stresses [24]. However if this process is taken too far the surface oxidised layer may spall off. In transformation toughened zirconia containing ceramics surface compressive stresses may be developed by grinding induced transformation of a surface layer, the depth and effectiveness of which increases with grinding severity [25]. It is also possible to destabilise the surface layer by chemically removing stabilisers and thereby enabling the volume expanding tetragonal to monoclinic phase change to take place on cooling leading to surface compressive stresses and increased strength [26].

The magnitude of such surface compressive stresses are given by the following simple relationship, namely

$$\sigma_R = \frac{\Delta V \, V_f \, E}{3 \, (1-\nu)} \tag{6}$$

where ΔV is the volume dilation, V_f the volume fraction of transformed phase, E Young's modulus and ν Poission's ratio.

3.2.2. Microcrack Toughening

Stress induced microcracking may take place in a range of single and polyphase ceramic microstructures that contain localised residual stresses. These residual stresses arise from thermal expansion anisotropy of non cubic polycrystalline materials, thermal expansion or elastic mismatch in poly phase materials and stresses arising from second phase inclusions that undergo a volume change due to a phase transformation upon cooling. Crack tip shielding results due to the instability of residually-strained regions in the near vicinity of the crack tip. This instability within a process zone results in micro cracking either circumferentially or radially (depending upon the internal stress within the second phase inclusion) or at a grain boundary in a single phase material. The critical size of grains or second phase particles for spontaneous cracking of such materials have been addressed in detail [27] and here we shall confine ourselves to subcritical sized materials that are triggered by the high tensile stresses about the crack tip. A schematic diagram of this mechanism is shown in Figure 6.
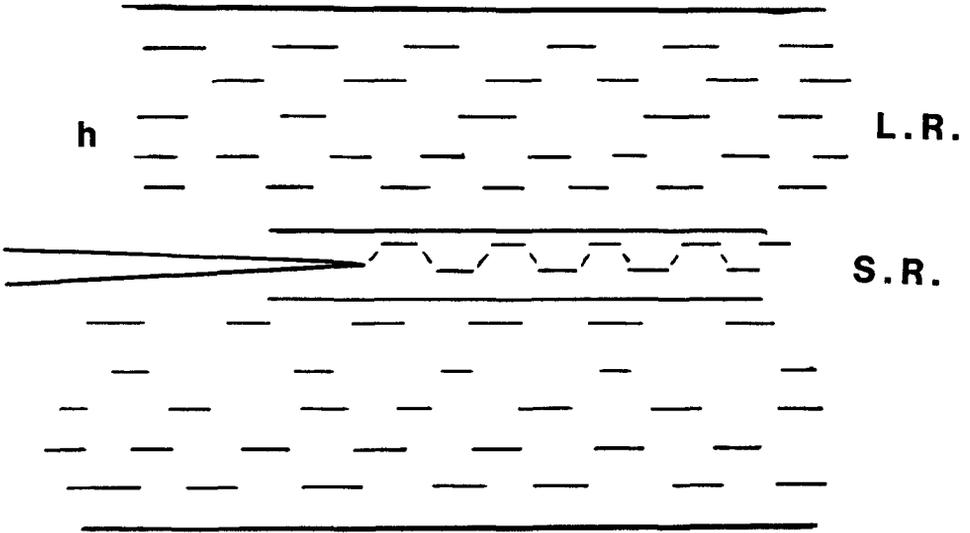
Figure 6.   Schematic diagram of a microcrackedzone about a macrocrack.
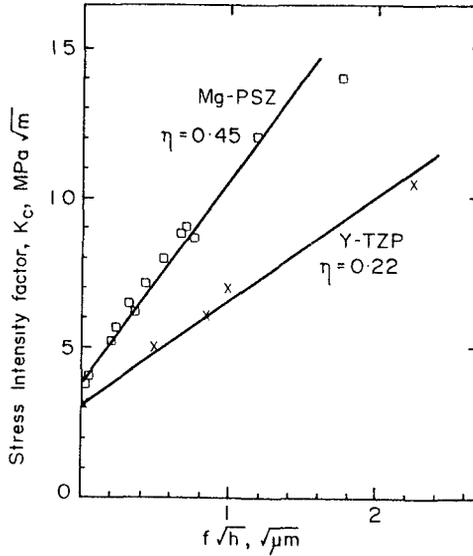

Figure 7.   Dependence of K_c of PSZ and TZP ceramics on dimensions of
             the transformation zone size and volume fraction of
             transformed monoclinic zirconia.

Two features that are important in these materials is that upon the initiation of microcracks in the process zone, permanent crack opening occurs at each microcrack and associated with this micro-cracking is a reduction of the elastic modulus within this zone. There is still considerable differences in the theoretical treatments of the toughening increment due to stress induced micro-cracking. Some authors have treated the problem analogous to transformation toughening with the additional feature of a reduction in elastic modulus [28]. Others have approached the problem as an energy disipation zone within which a crack linking region exists [29]. The former provides the simplist analysis and will be presented here. If we consider there is a critical stress to initiate microcracking and results in a volume strain of ϵ^M, the toughening increment maybe written

$$\Delta K^m = 0.21 \ E \ \epsilon^M \ h^{1/2} \ / \ (1-\nu) \tag{7}$$

where E is the Young's modulus, h the micro-crack zone heighe and ν is Poisson's ratio. The value of ϵ^M depends upon the conditions for micro cracking. For spheres under a residual tensile stress of σ_R, it has been shown that

$$\epsilon^M = 16 \ (1-\nu^2) \ \sigma_R V/ \ (3 \ E) \tag{8}$$

where V is the volume fraction of microcracking spheres. This leads to the expression

$$\Delta K^m = 1.12 \ V \ \sigma_R \ h^{1/2} \ (1 + \nu) \tag{9}$$

Whereas for spheres under internal pressure, leading to radial micro cracking

$$\epsilon^M = 2 \ \epsilon^T (V + [3V/4\pi]^{1/3}) \ /3 \qquad\qquad (10)$$

where ϵ^T is the dilational strain due to transformation strains or thermal expansion mismatch strains ($\Delta\alpha \ \Delta T$). Substitution of this expression into equation (6) provides an estimate of the toughening increment.

Unfortunately there is very little definitive experimental data on the toughening increment due to micro cracking zone width on the internal stress or size of the second phase particles. This situation also exists for coarse grained polycrystalline materials like alumina for which it has been proposed that micro cracking is the predominant mechanism. Data by Ruhle et al [30] for zirconia toughened alumina (ZTA) with a K_{1c} value of 6 MPa $\sqrt{m}$. indicates that the toughening contribution due to microcrack shielding is only 1 MPa $\sqrt{m}$. This estimate is in good agreement with both a theretical [31] and finits element analysis [32] of microcrack toughening. Very recent experiments by Lutz et al [33] with ceramic materials consisting of a matrix containing second phase spheres of known size and internal stress have provided definitive evidence of micro cracking and long range R-curve behaviour.

3.2.3 Transformation Tougheneing

This mechansims for improving the toughness of ceramics relies upon a stress assisted martensitic volume expanding phase change that takes place about the crack tip. It was first appreciated by Garvie et al [2]

in 1975 in zirconia partially stabilized (PSZ) ceramics. Zirconia
(ZrO_2) exists in three phases depending upon temperature, namely

$$\sim2300°C \qquad\qquad \sim1200°C$$

ZrO_2	ZrO_2	ZrO_2
(cubic)	(tetragonal)	(monoclinic)
$\rho = 6.09$gm/cc	$\rho = 6.10$	$\rho = 5.83$

The massive transformation strains, both dilational and shear, of the
tetragonal → monoclinic transformation cause destruction of articles
fabricated of pure zirconia. This feature is overcome by the addition
of various stabilizers such as MgO, CaO and various rare earth oxides.
Judicious selection of stabiliser content and sintering – heat treatment
conditions leads to retention of the tetragonal zirconia phase at room
temperature. Then the application of stress may lead to the following
reaction.

$$\text{stress}$$

$$ZrO_2 \text{ (tetragonal)} \qquad\qquad ZrO_2 \text{ (monoclinic)}$$

$$\text{heat}$$
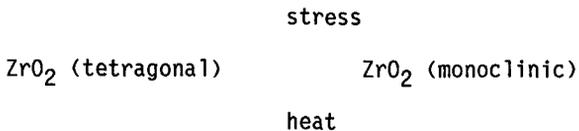
A wide range of microstructures containing tetragonal zirconia may
be fabricated varying in grain sizes from $0.2\mu m$ completely tetragonal
zirconia polycrystals (TZP) to $50\mu m$ grain size with lenticular
tetragonal precipitates in a cubic zirconia matrix in PSZ materials. A
third group containing tetragonal zirconia dispersed ceramics (ZDC) in
another matrix e.g. alumina, mullite etc [34].

A schematic drawing of the development of a transformed zone about a crack is shown in Figure 1 . Only in this instance the zone is under internal pressure resulting from the transformation. The toughening increments achieveable in transformation toughened materials have been discussed from the basis of energetics or mechanics perspectives [35,36]. To date the theoretical arguments have taken the materials as essentially isotropic with a smeared out zone of transformation about the crack tip area. More detailed models are required to fully appreciate the toughening mechanisms. Both approaches predict comparable relationships, and are of the form [37]

$$K_c = K_0 + \Delta K^T$$

(11)

and $\Delta K^T = \eta\ E^* e^T\ V_f \sqrt{h}$

where ΔK^T is the transformation toughening increment, K_0 the toughness of the matrix material, h the size of the transformation zone normal to the crack, e^T the dilational strain, E^* the effective modulus of the material and η a constant determined by the transformation zone shape. The effective modulus E^* as pointed out by McMeeking [38] plays a very important role in determining the effectiveness of the dilational strain of the zirconia phase (E ~210GPa, ν = 0.3) on that the matrix in ZDC materials. The influence of the dilation in an alumina matrix (E ~380GPa, ν = 0.2) is only one third as effective as in a PSZ material.

Substantial experimental support for the simple relationship in equation (11) has been obtained for a range of transformation toughened

ceramics both PSZ and TZP materials [39]. This is shown in Figure 7 which plots the toughness of 3 different systems, Mg-PSZ, Y-TZP and Ce-TZP against volume fraction and width of the transformed zone. The latter have been measured with a Raman microprobe system which enables volume fraction and zone width to be measured very accurately. The observations show that a five fold increase in toughness is possible in PSZ materials. The difference in slope (of value) of the Ce-TZP material from the other materials is suggestive of a different zone shape for the Ce-TZP material.

This is indeed found to be the case as shown in Figure 8 which compares the transformation zone about a crack in Mg-PSZ and Ce-TZP material [40]. The former is almost as predicted on the basis of a "small scale" transformed zone modified by anisotropy in various grains along the crack front. Whereas the zone shape in Ce-TZP material is closer to a craze zone in a polymer or Dugdale stretch zone in a metal. This similarity has been further explored to elucidate the basic transformation mechanisms in TZP materials [41].

Another parameter that significantly influences the toughness of transformation materials is temperature. With increasing temperature the tetragonal phase becomes more stable making transformation energetically more difficult and hence the zone size and toughness decreases. Recently Becher et al [42] have shown that the critical normalising parameter is the M_s temperature at which the tetragonal phase spontaneously transforms to the monoclinic phase. The toughening increment ΔK^T (equation 1) may then be modified to the following relation [42]
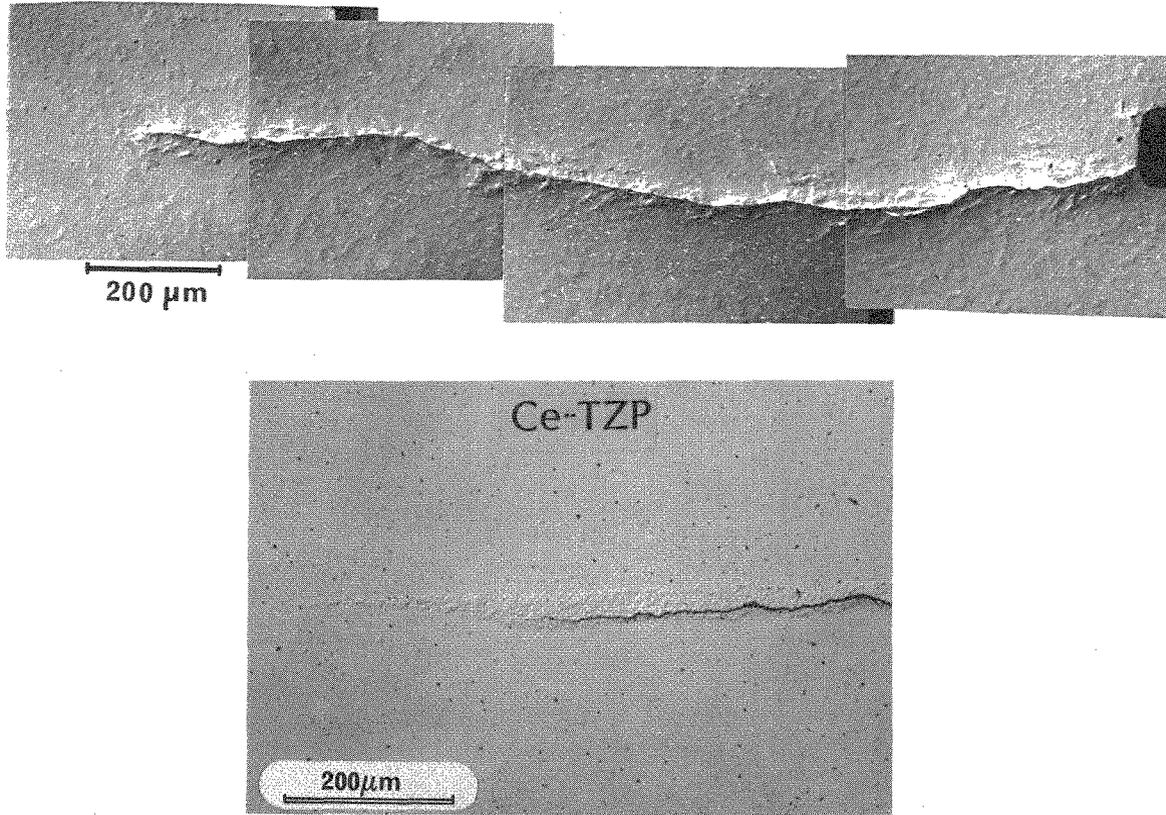
Figure 8.   Comparison of the transformation zones about the crack tip
in Mg–PSZ and Ce–TZP materials.

$$\Delta K^T = \frac{\Omega \, \eta (e^T)^2 \, V_f \, E \, K_o}{\Delta S \, (T - M_s)} \qquad (12)$$

where Ω and η are constants, ΔS is the entropy difference between tetragonal and monoclinic zirconia.

Experimental evidence in support of this expression is shown in Figures 9 which plot K_c versus temperature for Mg-PSZ materials [42], and a range of PSZ and TZP materials. The maxima in toughness corresponds with the M_s temperature and thereafter decreases linearly with temperature to the matrix K_o value. The realisation of the temperature sensitivity of transformation toughened ceramics has lead researchers to search for other less temperature sensitive toughening mechanisms to enable materials to have high toughness at temperature.

Recent studies have shown that it is possible to extend the analysis on which equation 2 is derived and predict the grain size dependence of the toughness of PSZ and TZP materials [43]. The approach combines the end point thermodynamic arguments developed by Garvie and Swain [44] and combines them with the fracture mechanics arguments of Evans and McMeeking [37]. This leads to the expression

$$\Delta K^T = \frac{\Omega \, \eta (e^T)^2 \, V_f \, K_o}{[< \Gamma.\tau + \sigma \, e > + \tau \, kd^{-\frac{1}{2}}]} \qquad (13)$$

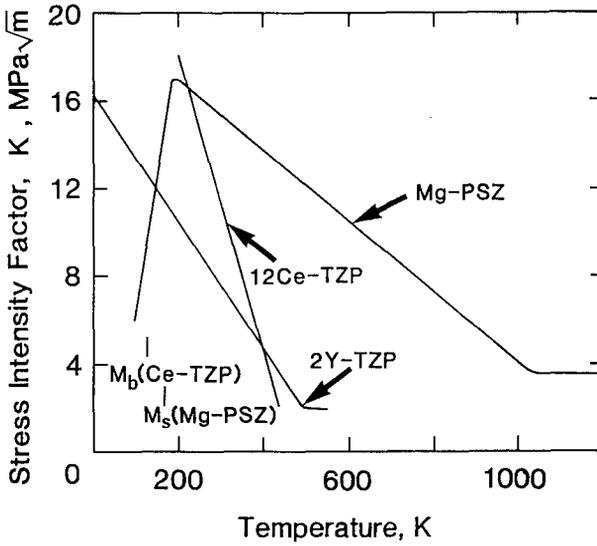where Γ_o is the single crystal transformation shear stress, k is a

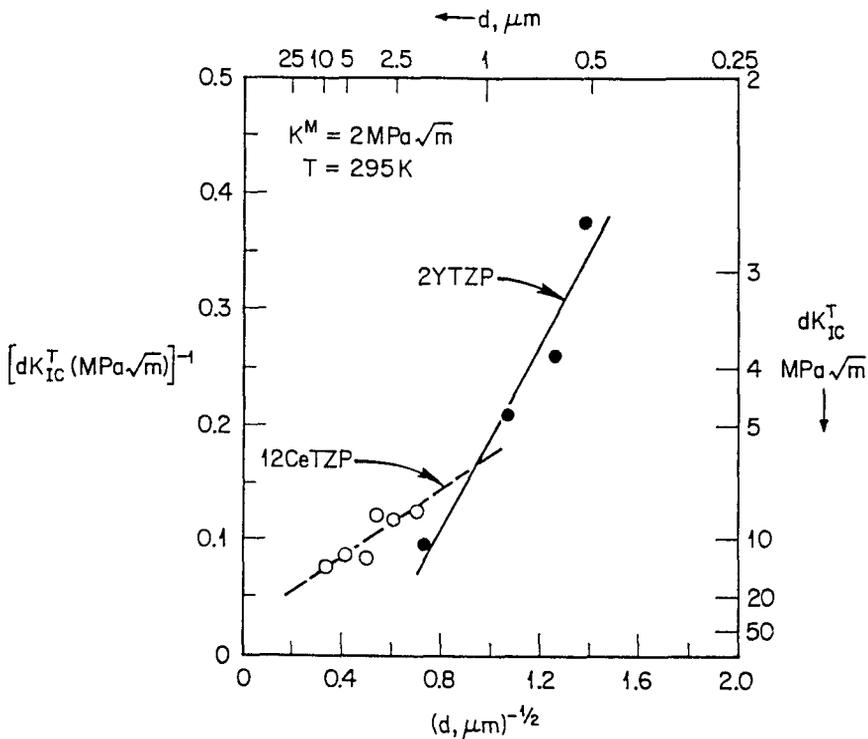Figure 9. Temperature dependenced of the toughness of a range of transformation toughened ceramics.

Figure 10. Grain size dependence of the toughness of Ce–TZP and Y–TZP materials.

constant, d is the tetragonal grain size, σ the applied stress and e the resultant strain. Evidence in support of this relationship is shown in Figure 10.

The fracture toughness as observed and predicted theoretically for transformation toughened materials exhibit R-curve behaviour [35, 45]. This occurs because the volume dilation provides closure forces behind the crack tip, the observed R-curves in PSZ materials are shown in Figure 11. The rise in toughness occurs over approximately 5 times the transformed zone height. This feature only becomes significant for materials with well developed transformed zones or materials with high K_c values. R-curves have been observed for Mg-PSZ and Ce-TZP materials directly with standard fracture mechanics tests, e.g. DCB and SENB, as well as optically on tensile surfaces of flexure bars [46,47,48]. Associated with such cracks are surrounding zones of transformed zirconia which are readily observed using interference microscopy. It is observed that the onset of crack growth takes place at lower values of K_{1c} for surface cracks than through thickness cracks [48]. For transformation toughened ceramics where the toughness maybe modified by heat treatment the consequences of R-curve predict a maxima in a plot of the strength versus toughness (steady state) [46,48].

Another feature of transformation toughened materials is their observed non-linear stress-strain relationships in tension and compression [49]. The inelastic deformation to failure is much greater in compression than tension. The onset of ductility occurs because of the metastability of the tetragonal phase and the dilation is associated with the transformation to monoclinic due to transformational
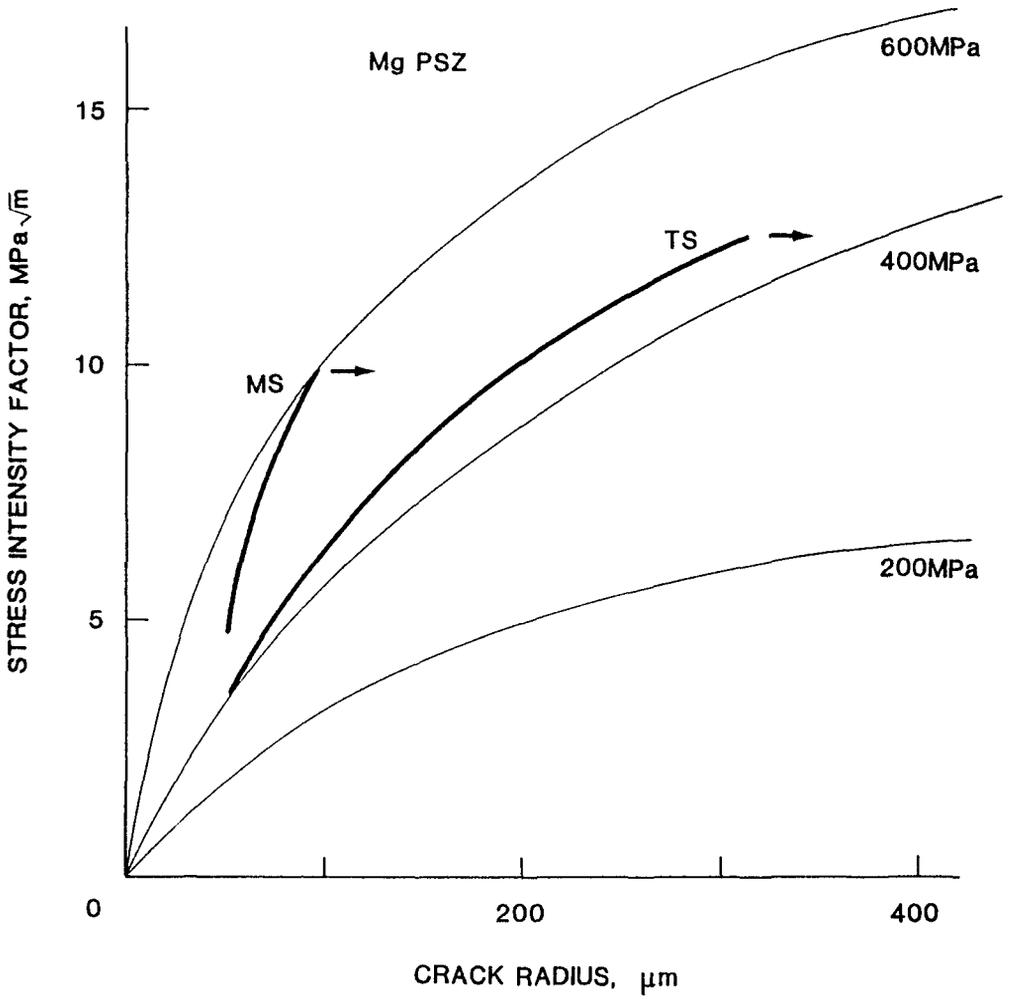
Figure 11. Observed R-curves in transformation toughened ceramics.

plasticity. This is determined by the M_s temperature which maybe modified by heat treatment, composition and grain size. In the PSZ materials the ductility takes place by means of a collaborative transformation of tetragonal precipitates often leading to microcracking at grain boundaries [50]. In TZP materials luders like bands are observed which occurs because of monoclinic laths are formed within tetragonal grains initiating adjacent grains [51]. The failure locus of a Ce-TZP material at room temperature due to stress induced transformation [52] is shown in figure 12. These observations are in excellent agreement with predictions of Chen and co-workers [53,54].

A consequence of the ductility of PSZ and TZP materials lead the author to propose an inverse relationship between strength and toughness [49]. Tougher materials such as Ce-TZP and also tough Mg-PSZ, "yield" prior to fracture. Also Y-TZP materials increase in strength with decreasing toughness initially. The inverse relationship proposed is shown in Figure 13. The highest strengths of 2.4 GPa are observed in hot isostatically pressed (HIP) specimens of Y-TZP containing 20-40 vol% Al_2O_3. The slope of the line through the origin indicates the critical flaw size to achieve such high strengths at a specific K_c value. For instance damage of the very high strength materials with a 10N Vickers indentation introduces flaws of approx. 200μm and the strength plummets to only 200 MPa. Whereas for Mg-PSZ material with a K_c value of 15 MPa$\sqrt{m}$, indents with loads as high as 500N causes no reduction in strength. More complete reviews of the Science and Technology of Zirconia Ceramics are available in three recent conferences devoted to this topic [55].
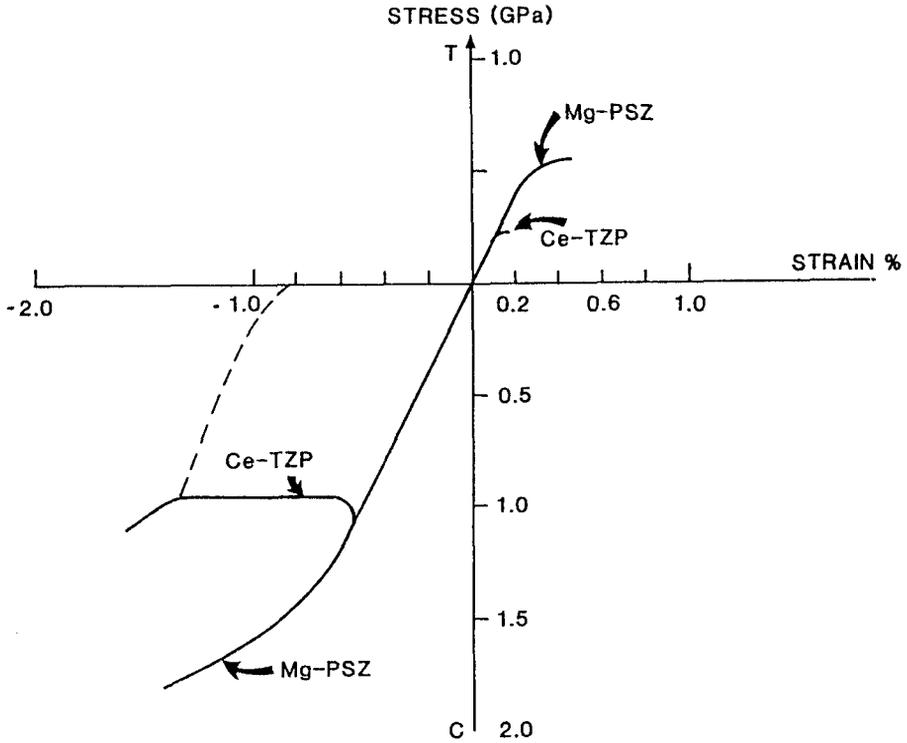
Figure 12. Stress Strain curves in tension/compression space for a 12 mol% Ce-TZP material and Mg-PSZ material.
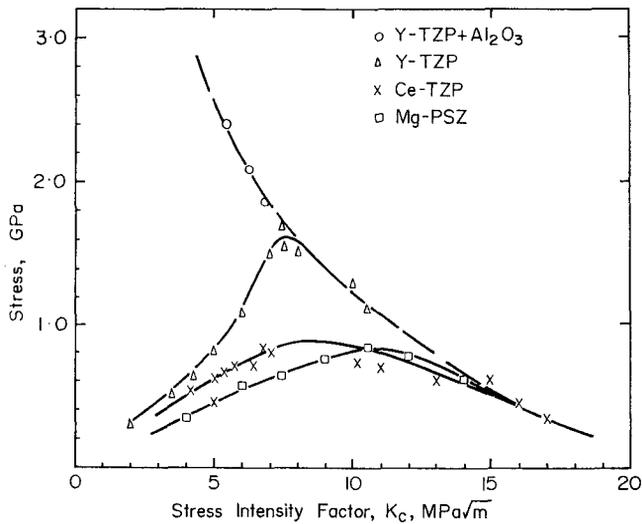

Figure 13. Strength-toughness relationships for several PSZ and TZP transformation toughened materials.

The most recent developments in the field of zirconia toughened ceramics include fabrication of composite zirconia — non oxide systems such as $TiB_2-ZrO_2(Y_2O_3)$ and similar types of materials [56]. These materials under specific atmospheres maybe sintered to near theoretical density and HIP'ed to achieve high strengths 1 to 1.5 GPa. Examples of the toughness hardness and strength dependence of such composites is shown in Figure 14. These materials are electrically conducting and maybe shaped using conventional electrical discharge machining (EDM) techniques. Two other interesting new developments in ZTC materials are the observation of superplasticity in TZP materials between 1100-1300°C enabling novel forming—forging techniques [57]. This behaviour plus the observation of shape—memory behaviour in PSZ and TZP materials [58,59] confirms the original description of "ceramic steel" for these materials.

3.3 Contact Shielding

Contact shielding as proposed by Ritchie [3] involves physical contact between mating crack surfaces. This situation occurs through the presence of fracture surface asperities, and crack tip bridging via fibres, metallic inclusions or frictional intenlocks caused by major crack deviation. The most effective mechanism of contact shielding is via fibre or whisker bridging of the crack tip. The latter is particularly attractive because of its similarity to conventional processing whereas continuous fibre reinforcement introduces complex ceramic fabrication routes that are currently very expersive.
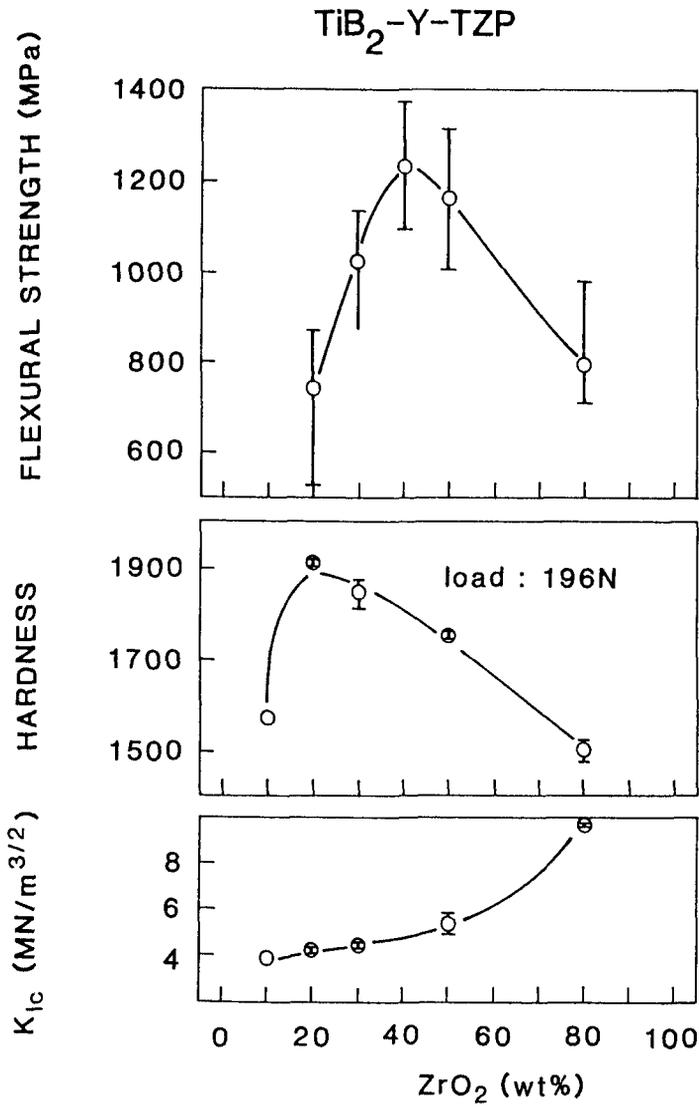
TiB$_2$-Y-TZP

Figure 14. Dependence of strength hardness and toughness of TiB$_2$-Y-TZP composites with composition.

3.31 **Whisker Reinforcment**

Almost two decades ago considerable interest was focussed on the preparation and properties of single crystal fibers or whiskers [29]. These materials are usually formed by vapour phase transport and preferential growth of certain crystal orientations. Because of their near perfect single crystal nature and fine diameters (μms) they exhibited in many instances near theoretical strength (> E/100). Interest in such materials as reinforcement for monolithic ceramics has resurged in the last three years. Most interest to date has centered on silicon carbide whiskers typically 0.5 – 1.0μm diameter and 100–200μm in length. Such materials are available from at least three suppliers although they tend to be very expensive ($200–500/kg).

A number of studies have shown that substantial improvements in strength, toughness and creep resistance maybe developed in polycrystalline ceramics by incorporating up to 20–30 volume % of whiskers [60,61,62]. The attractiveness of the types of materials is that they allow more conventional powder processing techniques to be used in fabrication. The initial approach was to fabricate by hot pressing of milled and blended compositions particularly alumina–silicon carbide. More recently emphasis has shifted towards being able to sinter/HIP such materials and obtain comparable mechanical properties [63].

Whisker reinforcement may involve a number of toughening mechanisms, such as, fibre pullout, crack bridging and crack deflection due to the high aspect ratio fibres. At this stage of the development and understanding of such materials it is difficult to quantify which

mechanisms are most effective. To date more attention has been placed upon the critical role of silicous layers on the whiskers leading to glassy films at the whisker—matrix interface. Such layers degrade properties above 800°C and lower the fracture toughness. For many whisker composites large thermal expansion coefficient (TEC) differences exist between whisker and matrix material with usually the TEC of the whisker < matrix. This leads to a clamping of whisker by the matrix making pullout more likely at higher temperatures, such behaviour is particularly, evident in mullite — silicon carbide whisker composites [64].

Becher et al [65] have recently proposed an analysis of the toughening contribution due to whisker reinforcement. The basis of their analysis is the development of the whisker bridging zone immediately behind the crack tip as a result of debonding of the whisker—matrix interface. Their analysis indicates the importance of the toughening increment upon composition and matrix, the interface and whisker properties. The approach adopted by these authors is to assume a Dugdale like crack tip zone where the increased toughness is associated with a closure stress on the crack by the bridging zone and a length of the zone. On the assumption of a uniform closure stress over the bridging zone the toughening increment is given by [65],

$$\Delta k^w = \sigma_f^w \left[\frac{V_f \quad r}{3 \ (1-\nu^2)} \quad \cdot \quad \frac{E^c}{E^w} \quad \cdot \quad \frac{G^m}{G^i} \right]^{\frac{1}{2}} \qquad (14)$$

Where $\sigma_f{}^W$ is the strength of the whiskers, E^C and E^W are the elastic modulus of the composite and matrix respectively, and G^m and G^i are the interfacial strain energy release rate of the matrix and interface respectively. This relationship highlights the importance of the strength, volume fraction, radius and elastic modulus of the fibres (whiskers). Evidence in support of the predictions of equation is shown in Figures 15 and 16. Figure is shows the dependence of the toughening increment on the square root of the volume fraction of whiskers, it also indicates the matrix modulus dependence as E mullite ~ 0.5 E alumina. The influence of whisker radius and interfacial toughness is shown in Figure 16. The higher toughness materials were treated prior to fabrication to remove the silica rich layer from the surface.

The strength of whisker reinforced alumina illustrating both the volume dependence and temperature dependence is shown in Figure 17. The strength shown a significant increase with volume fraction of whiskers in a manner similar to the toughness whereas only about 1000°C is their a significant decrease in strength.

The increase in strength with volume fraction of whiskers is partially due to a reduction in grain size. The creep properties of alumina—silicon carbide whisker materials are much improved over pure alumina [62].

One of the problems of whisker reinforcement of ceramics has been to obtain homogeneous distributions of the whiskers throughout the material. As fabricated whiskers usually are highly matted materials with clumps sometimes difficult to disperse. Such regions usually result in subsequent failure origins and may have remnant porosity about
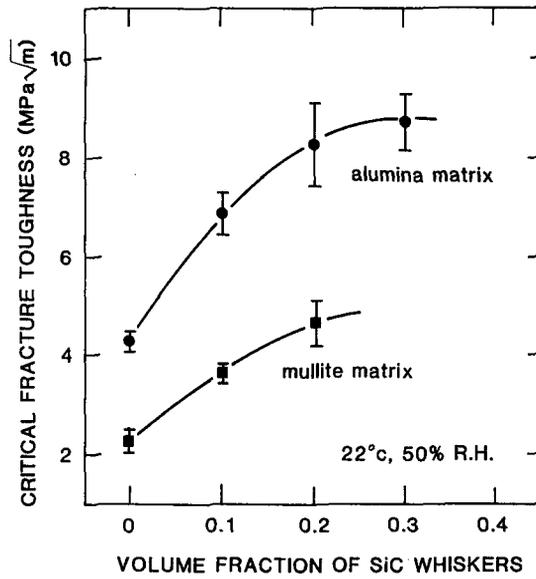
Figure 15.   Variation of the toughness of alumina and mullite with
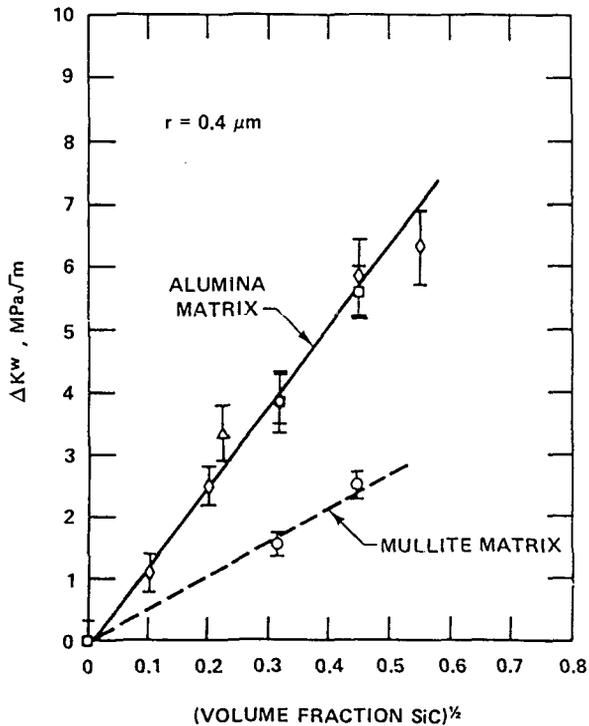volume fraction of SiC whiskers.

Figure 16.   Influence of whisker content on the strength of alumina –
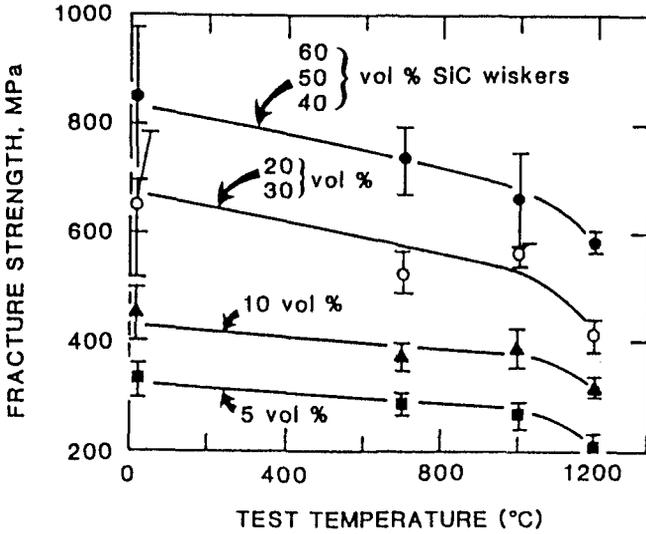silicon carbide whisker materials.

Figure 17. Strength of whisker reiforced alumina as a function of temperature and volume fraction of whiskers.

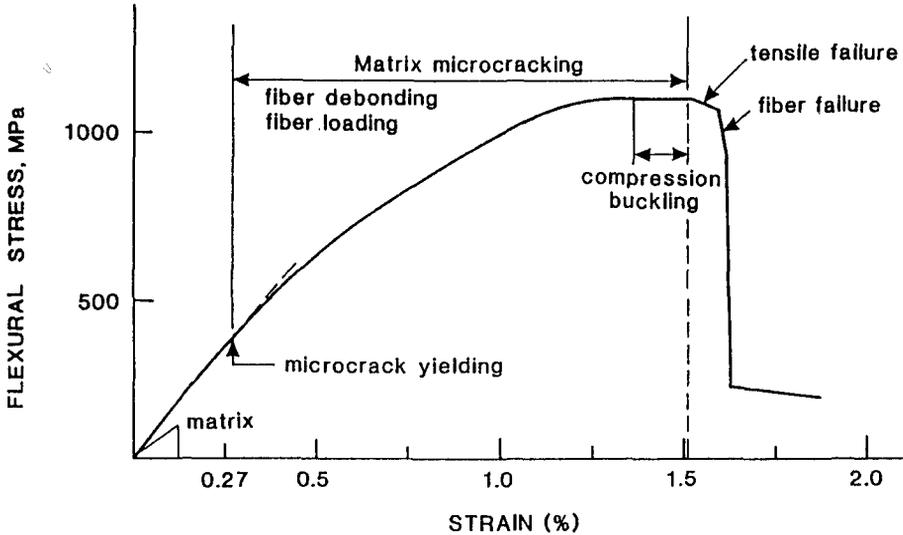SiC FIBER REINFORCED BMAS III GLASS-CERAMIC
(0°/0°, 30 VOL. %, 25°C)

Figure 18. Flexural stress – strain behaviour of a SiC fibre reinforced glass ceramic indicating deformation mechanisms that lead to changes in slope of the curve.

them. Alternate approaches for achievement of whisker like micro-structural reinforcement has been developed by other workers. For instance Tani et al [66] have found by sintering silicon nitride with small additions of alumina and yttria or ceria at up to 2000°C and an overpressure of nitrogen that large high aspect ratio β-silicon nitride grains develop. Such materials have K_c values double that of conventional equi-axed silicon nitride materials.

3.3.2 Fibre Reinforcement

The recent availability of strong high quality fibres of various ceramics has lead to a renewed interest in fibre reinforced ceramics. Again this area achieved considerable attention well over a decade ago [67] however at that time only good quality carbon and glass fibres were available. Such materials were not suitable for high temperature composites in oxidising atmospheres. A major breakthrough occured about 10 years ago when Yajima [68] fabricated continuous silicon carbide fibres with diameters 15-20μms . These materials begin to degrade at temperatures above 1000°C. A detailed discussion of the properties and oxidation behaviour at elevated temperature is given by Mah et al [69]. These authors point out that behaviour of isolated fibers in various atmospheres does not necessarily determine their behaviour in a composite material. The important parameters tend to be, refractoriness, compatability between fibre and matrix and composite fabricability.

A range of potential matrix materials includes various glasses and

glass ceramics, crystalline oxides, carbides, borides, nitrides, etc.
The most widely used matrices have been glass and glass ceramics because
of the relative ease of composite fabrication generally by low pressure
hot pressing techniques. Attempts to fabricate ceramic matrix –
continuous fibres have usually been unsuccessful because of the
difficulties of densification about the fibres. Such problems also
exaggerate thermal expansion mismatch cracking between matrix and
fibre. More recently, following procedures developed for carbon–carbon
fibre composites, infiltration by chemical vapour techniques as well as
by polymer precursors have been used for carbide, nitride and
oxycarbonitride matrices [70,71]. Chemical vapour infiltration can take
place above 1000°C leading to dense composites with closed porosity and
typically 80–85% theoretical density. A key parameter that maybe taken
advantage of in such a processing route is that a thin interface coating
maybe deposited on the woven structure prior to deposition of the
matrix. In this manner the interface properties of the matrix to fibre
maybe controlled and so determine whether genuine reinforcement occurs
resulting in stable fracture fibre fracture and pullout or catastrophic
fracture through the composite. Crack stability requires that the
interface is strong enough to transfer load from the matrix to the
fibres yet weak enough to fail preferentially prior to fibre failure.

The mechanical properties of fibre reinforced composites are
impressive. The stress – strain behaviour of these materials has a
closer resemblance to a metal than a ceramic. An more detailed example
of a flexural stress–strain curve in a composite of SiC fibres in a
matrix of barium osumilite are shown in Figure 18. The changes in the
stress–strain behaviour indicate processes taking place in the material

namely matrix microcracking followed by compression buckling just prior to fibre failure and reduction in load bearing capacity. Examples of the temperature dependence of strength and toughness of glass – ceramic – SiC fibres composite are shown in Figure 19. These materials are critically dependent upon the atmosphere and strain rate dependence at temperatures above 600°C, this is because of oxidation of thin layers of NbC at the interface changes the interface bonding between matrix and fibre [69,72].

More extreme values of toughness have been measured for SiC-SiC fibre composites fabricated by chemical vapour infiltration. Values of K_c as high as 39–40 MPa√m have been measured which are temperature insensitive to 1200°C [73]. An extremely steep R–curve has also been found. A consequence of such extreme toughness is that the material exhibits no reduction in strength upon thermal shock testing into water from temperatures as high as 1300°C. These materials response to crack extension are being addressed in a manner similar to that of tough metals which exhibit initial crack tip blunting prior to crack advance [74]. Work on such materials is currently limited by the high temperature degradation of fibres and the oxidation or creep response of the matrix. Attempts are underway to raise the operating temperature of such composites to 2000°C in air.

3.3.3 Crack bridging

As with all contact shielding toughening occurs due to events taking place behind the crack tip. As hinted at in section 3.2.2 (micro–crack toughening) many processes that were considered to generate a zone of micro cracks ahead of the crack tip. This situation was
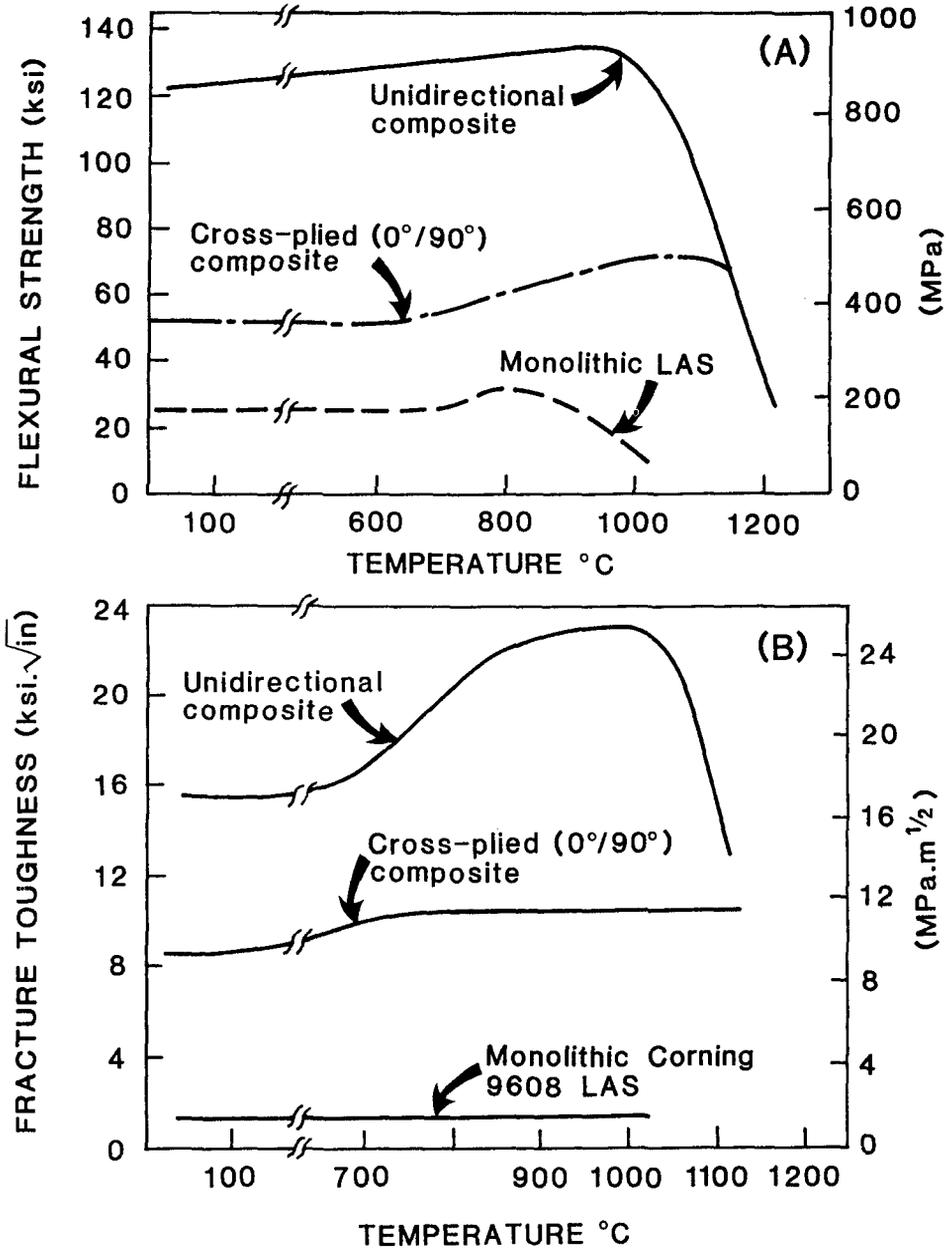
Figure 19. Temperature dependence of strength and toughness of SiC reinforced glass ceramic.

thought to occur in coarse grained alumina and other high thermally anisostropic materials. These materials were known to exhibit high steady state fracture toughness with considerable R-curve behaviour. However recent observations by Knehans and Steinbrech [75] and Swanson et al [76] indicate that events taking place at large distances behind the crack tip are responsible for a major part of the toughening. Knehans and Steinbrech [75] were able to definitively show that events behind the crack tip were responsible for the toughening by re-notching to just behind the crack tip, this lead to a significant reduction in the fracture toughness and re-development of the R-curve with further crack extension. Optical and scanning electron microscope observations confirm that frictional (mechanical) interlocking events generate closure forces behind the crack tip and are responsible for the increased toughness. Analysis of the problem has been very difficult as it is virtually impossible to estimate the force-displacement (stiffness) of these crack bridges and so estimate the closure forces.

Examples of the frictional interlock events taking place along a crack in a three phase TiB_2 based aluminium evaporator boat material [76] are shown in Figure 20. This material exhibits a significant R-curve behaviour, the range of which scales with the extent of crack bridging events behind the crack tip. Observations of the crack opening displacement with distance behind the crack tip for the material in Figure 20 were found to exhibit an inflection at the end of the bridging region.

Other mechanisms of crack bridging in ceramics is by the incorporation of a ductile phase into the matrix. These materials, one example of which has been the WC base hardmetals,
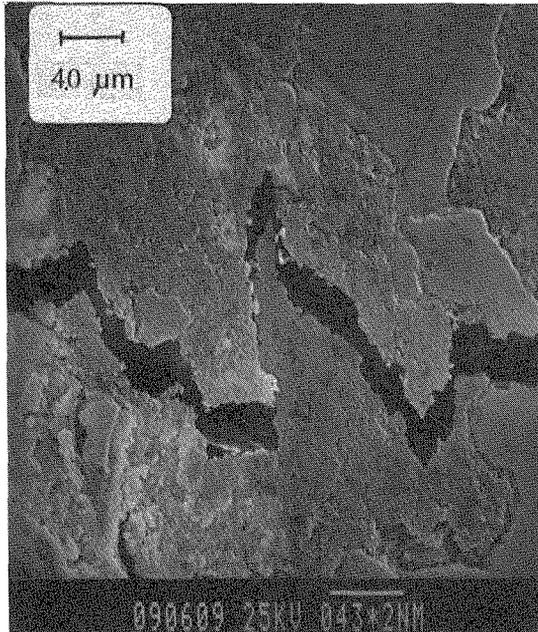
Figure 20. Observations of regions of frictional interlock in a TiB_2
based aluminium evaporator boat.

4 Strength in Service

The maintenance of strength, or understanding of factors controlling its degradation of in service, is one of the major considerations of current ceramic materials research. Considerable attention over the last decade has been given to the parameters that are important for the nucleation of cracks through contact with sharp or blunt indenters and in abrasion and machining operations [78,79]. This has entailed a detailed understanding of deformation and contact fracture mechanics and has lead to simple indentation techniques being routinely used to characterise K_c values of materials. Other studies have explored the influence of defect shape, modulus and thermal expansion mismatch of inclusions on the resultant strength. The other key issue has been the influence of environment on slow crack growth resulting in failure of a component sometime after loading. These areas are reasonably well understood and procedures exist to enable design of ceramic structures within well defined safety limits or probabilities [80].

4.1 Fatigue

A number of key areas in the field of mechanical behaviour of ceramics still require considerable attention. They include the influence of cyclic loading on the lifetime of a structure and measurement of simple S–N curves. This becomes particularly important

for crack tip shielded toughened materials or those that exhibit non-linear stress-strain behaviour prior to fracture. Ritchie [3] has provided guidelines for the anticipated behaviour of crack tip shield materials response to cyclic loading. These features are shown schematically in Figure 21. For contact shielding the anticipated response is that the da/dN versus ΔK curve is shifted to higher ΔK values. With zone shielding, such as transformation or microcrack toughening the threshold value is barely affected but a less steep shape is expected which is exactly opposite to the influence expected for contact shielding. Evidence in support of these mechanisms is well accepted in the metals fraternity and is beginning to be more appreciated for ceramics. For instance in Mg-PSZ materials the lifetime predictions based upon static loading greatly overestimate the observations of lifetime under cyclic loading [81]. This is shown in Figure 22. The reason for this difference has recently been shown to be due to a genuine fatigue crack growth behaviour in PSZ materials with a slope much less than seen for static fatigue loading [82], Figure 23. Similar behaviour might be anticipated for fibre composite materials for stresses exceeding the onset of matrix-microcracking [6].

The other area where serious problems arise is in the area of high temperature application. At elevated temperatures ceramic materials are no longer chemically or physically stable. Chemical reactions between ceramics and the environment lead to the formation of new populations of flaws and or result in chemical or physical modification of the ceramic microstructure. All these processes may result in strength degradation
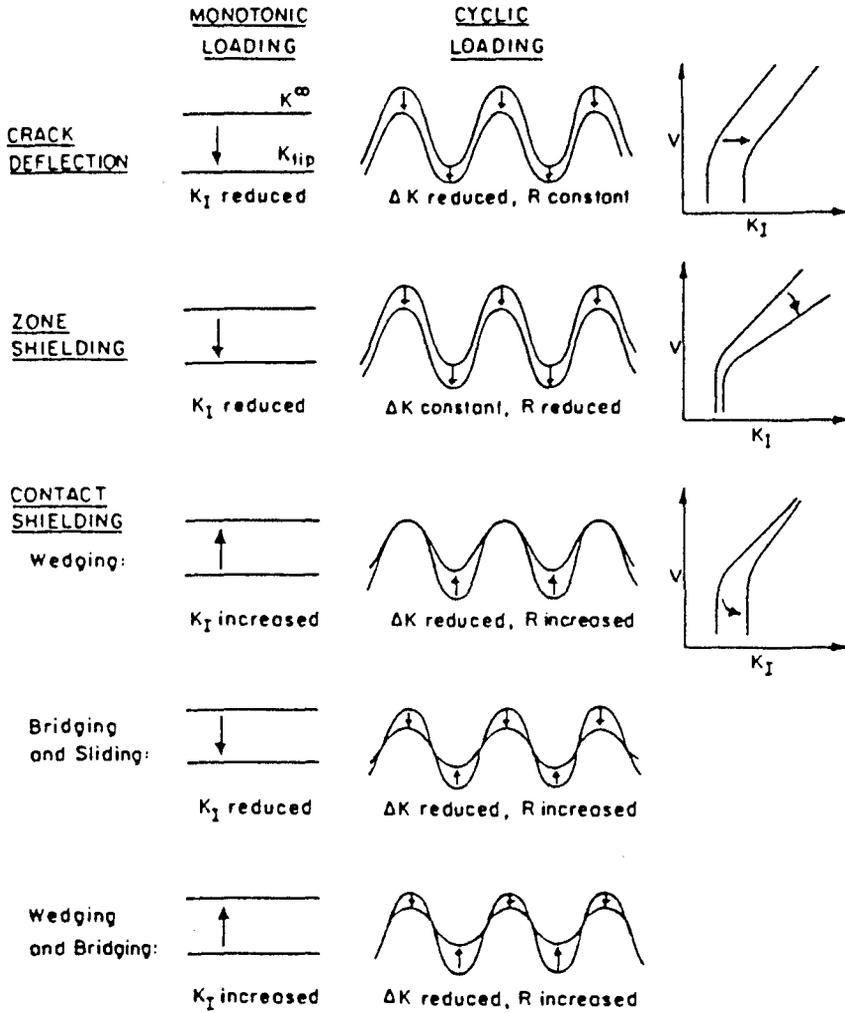
Figure 21.   Influence of specific crack tip shielding mechanisms on the driving force, ΔK and crack velocity on cyclic loading.
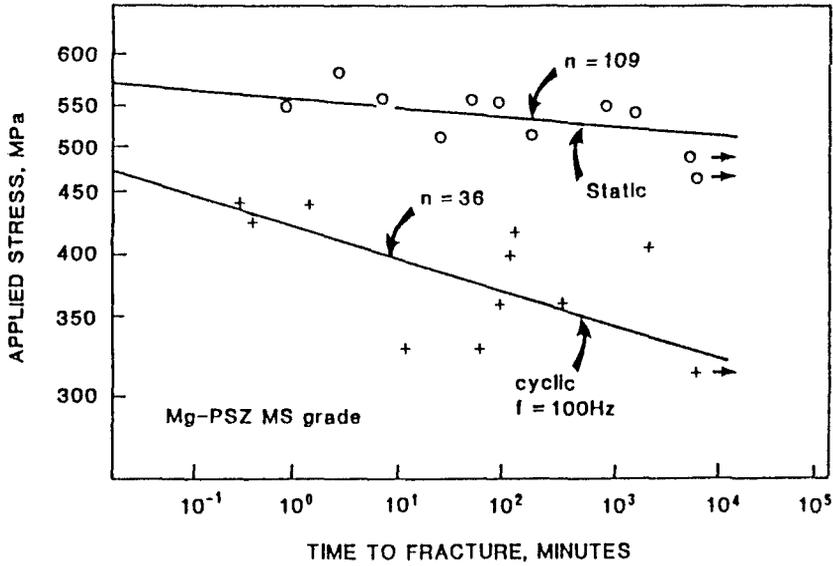
Figure 22. Comparison of lifetimes of Mg-PSZ tested under static and rotational cyclic flexural loading with applied stress.
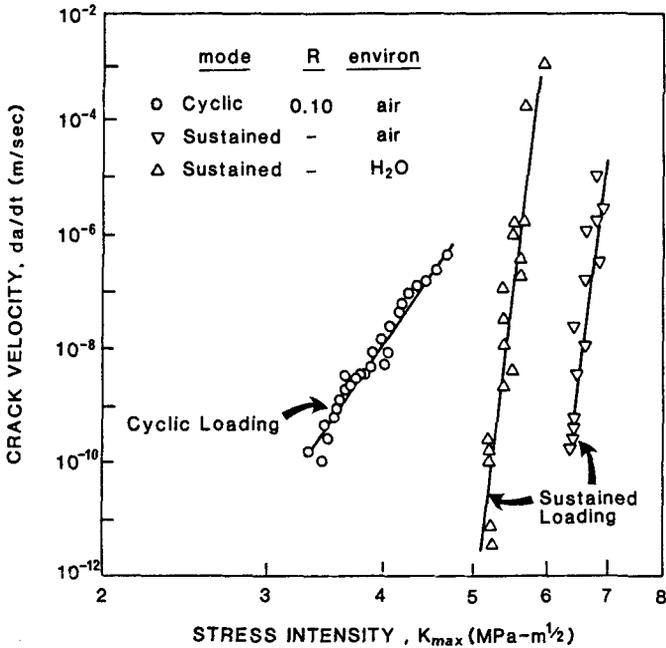

Figure 23. Comparison of the crack propogation rates with applied stress intensity factor for Mg-PSZ under static and cyclic testing conditions.

in service. Transport processes such as bulk diffusion or viscous flow
of a grain boundary phase are highly temperature dependent. Hence crack
nucleation and growth are observed to occur at elevated temperatures in
oxide and non-oxide ceramics as a result of creep. In this manner flaw
populations are generated in the material with time, leading to
mechanical failure of a component [83].

Attempts to understand behaviour of materials at elevated
temperatures are still very much at the experimental stage. Quinn [84]
has generated a fracture map for silicon nitride at elevated
temperatures, this is shown in Figure 24. These observations are for
the lifetime of static loaded silicon nitride (MgO doped) that been
given a 16N Knoop indentation prior to testing in order to reduce
scatter of the results. These observations and others in alumina [85],
and silicon carbide [86], suggest that, for short periods of time,
failure occurs by crack growth from pre-existing flaws.
At lower stresses and higher temperatures failure is controlled by creep
fracture processes. These results have been found to fit empirically
derived creep fracture relationships for metals, the Monkman-Grant
equation (namely $t_f \epsilon^{\alpha} = \beta$, where ϵ is the minimum creep rate,
β and α constants), or modified such relationships. Hence for a
particular material data must be obtained to determine the mechansims of
failure. Parametric relationships may then be obtained which provide
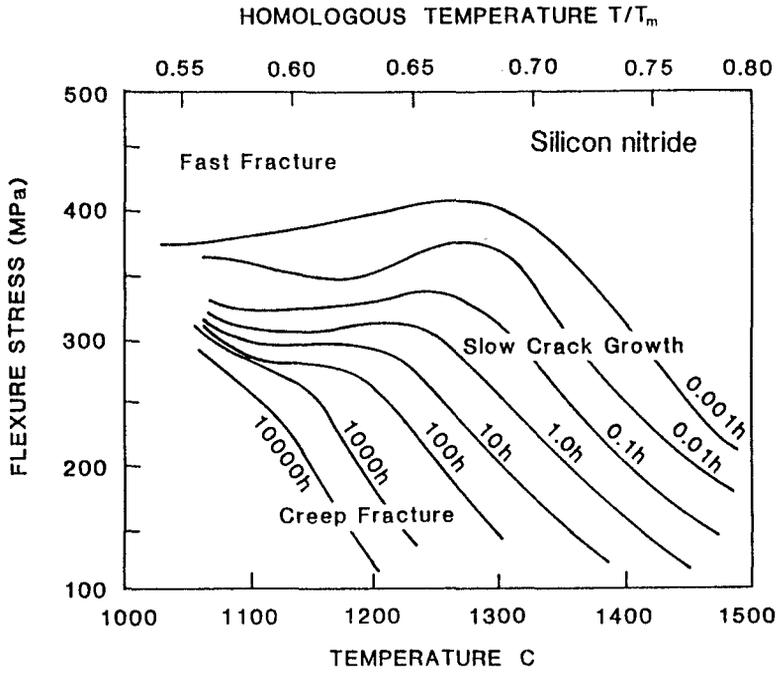the basis for structural design.

Figure 24. Fracture – mechanism – lifetime map of silicon nitride at
            temperatures where creep becomes significant.

5. FABRICATION DEVELOPMENTS

Associated with recent advances in the toughening mechanisms available to ceramics has been associated developments in the area of ceramic powder production and consolidation. Many of the processes are not novel but equipment and techniques are readily available or sufficiently well understood to be utilized on semi-production/commerical basis.

Until recently most ceramic processing consisted of familiar milling of powders to achieve particle sizes that may be sintered with or without the assistance of sintering aids. Such processing even with the advent of more rapid attrition milling systems was time consuming and introduced many steps where contamination was inadvertantly introduced into powder. A number of processes are now available that completely eliminate such milling/mixing procedures and result in greatly improved purity of powders and performance of products. A listing of such processes (not meant to be exhaustive) includes,

Sol—gel (aero—gel)

Polymer precursors

Melt processing — rapid quenching

Chemicl reaction deposition (plasma, laser)

Chemical vapour deposition/infiltration

Extensive reviews of the progress possible in these areas may be found in two recent MRS conference proceedings and elsewhere [87]. The usual problem with many of these techniques is that the cost of powders

produced is much greater than by current production methods, and as mentioned this factor limits penetration of ceramics in the highly cost competitive automotive engine market. Where these alternate processes are making a significant impact is in the area of highly refractory materials such as carbides and borides. Plasma chemical reaction techniques have been used to fabricate highly sinter active powders of titanium diboride with incorporated sintering aid and grain growth inhibition (carbon) into powders typically $0.1 - 0.4\mu m$ diameter. These materials may then be sintered to near theoretical density at temperatures as low as 1700°C — a feat not possible by traditional techniques [88]. Other advantages of such an approach to powder fabrication is that it enables homogenous solid solutions of various species and so develop complex precipitate laden highly refractory materials.

Although chemical vapour deposition (CVD) may appear as an expensive route to fabricate monolithic components it does offer some unique advantages. Materials maybe fabricated over a range of compositions at reasonably rapid deposition rates and variable crystallinity. Hirai and colleagues [89] have shown that CVD materials have exceptionally clean grain boundaries that improves the oxidation resistance of silicon nitride materials by at least 200°C over that of sintered materials. Other modifications in processing enable fibre like microstructures to be developed and the density of stacking faults to be modified, both means of increasing the fracture toughness [90].

The recent widescale availability of hot isostatic pressing (HIP) facilities with operating conditions exceeding 2000°C and 200 MPa has been another great means for improvement of the strength of ceramics.

The most spectacular examples of this have been in the area of zirconia toughened ceramics where strengths up to two times that achievable by conventional sintering are possible [91]. However HIP'ing may lead to the undesirable introduction of carbon into the ceramic. This is observed in zirconia ceramics when HIP'ed in argon atmospheres with carbon heating elements. This aspect is discussed elsewhere and at this conference [92]. The most recent vintage HIP facilities provide for oxygen containing atmosphere up to 1500-1600°C. Another advantage of such an approach is that a range of oxides may now be fabricated to near transparency.

With the appreciation that superplasticity is possible in fine grained ceramic materials the opportunity for a range of shaping techniques more usual considered for metallic materials such as forging becomes possible [57].

The future direction in processing and fabrication of ceramics is likely to follow in some instances along similar directions to metals processing. That is, greater emphasis placed upon solid solution/melt processing followed by heat-treatment precipitation processing as currently applied to PSZ materials. Already the literature on TTT curves for the development of various phases and the role of dopants in PSZ ceramic is available [93,94]. The other direction will be the greater emphasis placed upon coating technology to assist in overcoming the problems of high temperature oxidation/erosion/corrosion currently experienced by all non oxide materials. Already such approaches are being utilized in the fabrication of continuous fibre composite structures.

6. Conclusions

It is now well established at the research, technology, applications and production that a number of very effective toughening mechanisms are available for ceramics. Unfortunately mosts of these mechanisms are appropriate at lower temperatures as they are intrinsicelly temperature sensitive. The two exceptions would appear to be crack deflection toughening and whisker reinforcement, and even these have not been shown to be applicable in any materials at 1400°C or above.

The concept of crack tip shield provides a framewwork within which to analyse most of the effective toughening mechanisms. As a corrolary it also provides the basis upon which the more severe cyclic fatigue behaviour may be explained or possibly designed for. Current research attention is focussed on this area of fatigue crack growth and it is anticipated as with metallic materials that short cracks will initiate at much lower thershold cyclic stressing levels than longer cracks.

The major new ceramic materials initiatives would appear to be in the design of complex composite materials with a number of incorporated toughening mechanisms. These mechanisms would be anticipated to operate at different length scales from the nanometer to the millimeter range depending upon the size and application of the material. Increasingly novel and radical fabrication routes will be used to develop these complex microstructured composites.

REFERENCES

1. See for example Report by D.W. Lee of Arthur Little Inc. (Nov.
    1986) similar estimates have been proposed by Kline, SRI and other
    market forecasting bodies.

2. R C Garvie and R H J Hannink and R T Pascoe: Nature, Vol 258, 703
    (1975)

3. R.O. Ritchie Mat. Sci and Eng in press (1988)

4. Y. Matsuo and S. Kimura J. Ceram. Soc Japan, Int. Edt 96 C-125
    (1988).

5. A Kelly: "Strong Solids" Clarendon Press (1966).

6. D Munz et al: Fracture Mechanics of Ceramics Vol 7, p 265 1986,
    Plenum Press N.Y. Edts. R C Bradt, A G Evans, D P H Hasselman and F
    F Lange.

7. E. Orowan Rept. Prog. Phys. 12, 185 (194a)

8. Y.W. Mai and B.R. Lawn Ann. Rev. Mater. Sci. 16, 415 (1986).

9. B. R. Lawn and S. Lathabai to be published.

10. M V Swain and L R F Rose: "Advances in Fracture Research" Vol 1, p
    473 ICF 6. Edts. S R Valluri et al. Pergamon (1984).

11. M. Sakai and R.C. Bradt. J. Ceram. Soc. Japan 96, 779 (1988).

12. K. Kendall, N. Mc Nalford, S.T. Tan and J.D. Brichall J. Mater.
    Res. 1, 120 (1986).

13. R.F. Cook and D.R. Clarke Acta Met 36, in press (1988).

14. R.F. Cook, B.R. Lawn and C.J. Fairbanks J. Am. Ceram. Soc. 68, 604 (1985).

15. D B Marshall and J E Ritter: Bull. Am. Ceram. Soc. Vol 66, [2] 309 (1987).

17. K.T. Faber and A.G. Evans Acta Metal 31, 565 (1983).

18. K.T. Faber and A.G. Evans Acta Metal. 31, 577 (1983).

19. F.F. Lange, Bull Am. Ceram. Soc. 62, 1369 (1983).

20. S. Hori, H. Kaji, M. Yoshimura and S. Somiya MRS proceedings Vol. 78, 283 (1987).

21. M.V. Swain J. Mater. Sci. 16, 151 (1981).

22. B.R. Lawn and D.B. Marshall Phys. Chem. Glasses 18, 7 (1977).

23. H. Kirchener, R.E. Walker and D.R. Platts J. Appl Phys. 42, 3685 (1971).

24. F.F. Lange J. Am. Ceram. Soc. 63, 38 (1980).

25. M.V. Swain J. Mater. Sci. 15, 1577 (1988).

26. D. Green J. Am. Ceram. Soc. 66, c-178 (1983).

27. D.J. Green J. Am. Ceram. Soc., 64, 138 (1981).

28. A.G. Evans and K.T. Faber J. Am. Ceram. Soc. 67, 255 (1984).

29. W. Pompe and W. Kreher Adv. in Ceramis Vol, 12, 283 (1984).

30. M. Ruhle, A.G. Evans, R.M. McMeeking, P.G. Charalambides and

J.W. Hutchinson Acta Met. 35, 2701 (1987).

31. J.W. Hutchinson Report No. Mech — 87 Division of Applied Sciences, Harvard University. Comb. Mass. (1986).

32. P.G. Charalambides and R.M. McMeeking J. Am. Ceram. Soc. 71, 465 (1988).

33. E. Lutz, N. Claussen and M.V. Swain unpublished work (1988).

34. D.J. Green, R.H.J. Hannink and M.V. Swain. "Transformation Toughening of Ceramics" CRC in press 1988.

35. D.B. Marshall, A.G. Evans and M. Drory, Fract. Mechs of Ceramics Vol 6. p 289 Plenum N.Y. 1983.

36. B. ·Budiansky, J. Hutchinson and J. Lambropulos. Int. J. Solids and Structures 19, 337 (1985).

37. R.M. McMeeking and A.G. Evans. J. Am. Ceram. Soc. 65, 242 (1982).

38. R.M. McMeeking. J. Am. Ceram. Soc. 69, C-301 (1986).

39. P.F. Becher and M.V. Swain unpublished work 1987.

40. M.V. Swain, R.H.J. Hannink and J. Drennan, Ceramic Microstructures — 86. Mater. Res. soc. Vol. 21, 819 (1987) Plenum Press N.Y.

41. L.R.F. Rose and M.V. Swain Acta Metal 36, 955 (1988).

42. P.F. Becher, M.V. Swain and M.T. Ferber J. Mater. Sci, 22, 63 (1987).

43. P.F. Becher and M.V. Swain in preparation.

44. R.C. Garvie and M.V. Swain, J. Mater Sci., 20, 1193 (1985).

45. M.V. Swain and R.H.J. Hannink Adv. in Ceramic 12, 225 (1983).

46. M.V. Swain and L.R.F. Rose J. Am. Ceram. Soc. 69, 511 (1986).

47. D.B. Marshall J. Am. Ceram. Soc. 69, 173 (1986).

48. D.B. Marshall and M.V. Swain J. Am. Ceram. Soc. 71, 399 (1988).

49. M.V. Swain Acta Metal. 33, 2083 (1985).

50. R.H.J. Hannink and M.V. Swain J. Mater. Sci., 16, 1428 (1981).

51. R.H.J. Hannink and M.V. Swain J. Am. Ceram. Soc., in press 1988.

52. D. Shetty and K. Wu, J. Am. Ceram. Soc. in press.

53. I. Weh Chen and P.E. Reyes Morel J. Am. Ceram. Soc., 69, 181 (1986).

54. I. Weh Chen and P.E. Reyes Morel, Mat. Res. Soc Symp., Proc. Vol. 78, 75 (1987).

55. Adv. in Ceramics Vol. 3   (1981)
    ibid   Vol. 12 (1984)
    ibid   Vol. 24 (1988)
    Am. Ceram. Soc.

56. K. Shobu, J. Watanabe, J. Drennan, R.H.J. Hannink and M.V. Swain Adv. in Ceramics 24, in press 1988.

57. F. Wakai, S. Sakaguchi and Y. Matsuno Adv. in Ceramic Mater 1, 33 (1986).

58. M.V. Swain Nature (Lord) 322, 234 (1986).

59. A.P. Levitt "Whisker Technology" Wiley-Interscience (1970).

60. P.F. Becher and G.C. Wei, J. Am. Ceram. Soc. 67, C-267 (1984).

61. S.T. Buljan, J.G. Baldoni and M.L. Huckakeee, Bull Am. Ceram. So. 66, 347 (1987).

62. A.H. Chokski and J.R. Porter. J. Am. Ceram. Soc. 68, C-144 (1985).

63. T.N. Tiegs and P.F. Becher, Bull. Am. Ceram. Soc. 66, 339 (1987).

64. M.C. Shaw and K.T. Faber Materials Science Res. Vol 21, 929 (1987) Plenum Press N.Y.

65. P.F. Becher, C.H. Hseuh, P. Angelini and T.N. Tiegs, J. Am. Ceram. Soc 71, in press (1988).

66. E. Tani, J. Mat. Sci. Lett. 4, 1454 (1985)

67. R.A.J. Sambell, D.H. Bowen and D.C. Phillips J. Mater, Sci. 7, 663 (1972), 676 (1972).

68. S. Yajima, K. Okamura, J. Hayaski and M. Omoni J. Am. Ceram. Soc. 59, 324 (1976).

69. T. Mah, M.G. Mendiratta, A.P. Katz and K.S. Mazdiyasni Bull. Am. Ceram. Soc. 66, 304 (1987).

70. J.W. Warren, Ceram. Eng. and Sci. Proc. 6, 684 (1985).

71. A.J. Caputo Bull. Am. Ceram Soc. 66, 368 (1987).

72. K. Prewo and J. Brennan. J. Mater. Sci. 15, 463 (1980) 17, 1201 (1982).

73. P.J. Lamicq et al. Bull Am. Ceram. Soc. 65, 336 (1986).

74. M. Gomina Frac. Mech. Ceram. 7, 17 (1986) Plenum Press N.Y.

75. R. Knehans and R. Steinbrech J. Mater. Sci. 1, 327 (1982)

76. P.L. Swanson, C.J. Fairbanks, B.R. Lawn, Y.W. Mai and B.J. Hockey
    J. Am. Ceram. Soc. 70, 279 (1987).

77. M.K. Bannister and M.V. Swain, Materials Science Forum Vol. 34-36
    669 (1986).

78. B.R. Lawn, A.G. Evans and D.B. Marshall J. Am. Ceram. Soc., 63, 574
    (1980).

79. B.R. Lawn Fract. Mechs. Ceram. 5, 1 (1983) Plenum Press N.Y.

80. S.M. Weiderhorn, S.W. Freiman, E.R. Fuller and J. Richter ASTM
    Spec. Publ. 884, p 95 (1984).

81. M.V. Swain and V. Zelizko, Adv. in Ceramics 24, in press (1988).

82. R.H. Dauskardt, W. Yu, and R.O. Ritchie, J. Am. Ceram. Soc. 70, C-
    248 (1987).

83. S.M. Weiderhorn and E.R. Fuller. Mat. Sci. and Eng. 71, 169 (1985).

84. G.D. Quinn ASTM STP 884 p 177 (1984).

85. S.M. Johnson, B.J. Dalgleish and A.G. Evans J. Am. Ceram. Soc. 67,
    759 (1984).

86. S.M. Weiderhorn et al "Tailoring Multiphase and Composite
    Ceramics". p 755 Plenum Press N.Y. (1986).

87. "Better Ceramics Through Chemistry" MRS Symp. Proc. Vol. 32 (1984)
    Vol. 73 (1986).

88. H.R. Baumgartner and R.A. Steiger, J. Am. Ceram. Soc., 67, 207
    (1984).

89. T. Hirai Mat. Sci. Res. <u>17</u>, p 329 (1984) Plenum Press N.Y.

90. K.Niihara, A. Suda and T. Hirai, Ceramic Components for Engines p. 480 (1983) Edt S. Somiya et al KTK. Tokyo.

91. K. Tsukuma et al J. Am. Ceram. Soc. <u>68</u>, C–56 (1985).

92. C.L. Hogg, R.K. Stringer and M.V. Swain J. Am. Ceram. Soc., <u>69</u>, 248 (1986).

93. R.R. Hughan and R.H.J. Hannink, J. Am. Ceram. Soc., <u>69</u>, 529 (1986).

94. C.A. Leach. J. Mater. Sci. Lett. <u>6</u>, 303 (1987).